

Milky Way type galaxies in a Λ CDM cosmology

Maria E. De Rossi^{1*}, Patricia B. Tissera¹, Gabriella De Lucia² and Guinevere Kauffmann²

¹ *Instituto de Astronomía y Física del Espacio (Conicet-UBA), Argentina, CC67 Suc28, Buenos Aires (1428), Argentina.*

² *Max-Planck-Institut für Astrophysik, Karl-Schwarzschild-Str. 1, D-85748, Garching, Germany.*

29 January 2009

ABSTRACT

We analyse a sample of 52,000 Milky Way (MW) type galaxies drawn from the publicly available galaxy catalogue of the Millennium Simulation with the aim of studying statistically the differences and similarities of their properties in comparison to our Galaxy. Model galaxies are chosen to lie in haloes with maximum circular velocities in the range 200–250 km s^{−1} and to have bulge-to-disk ratios similar to that of the Milky Way. We find that model MW galaxies formed ‘quietly’ through the accretion of cold gas and small satellite systems. Only ≈ 12 per cent of our model galaxies experienced a major merger during their lifetime. Most of the stars formed ‘in situ’, with only about 15 per cent of the final mass gathered through accretion. Supernovae and AGN feedback play an important role in the evolution of these systems. At high redshifts, when the potential wells of the MW progenitors are shallower, winds driven by supernovae explosions blow out a large fraction of the gas and metals. As the systems grow in mass, SN feedback effects decrease and AGN feedback takes over, playing a more important role in the regulation of the star formation activity at lower redshifts. Although model Milky Way galaxies have been selected to lie in a narrow range of maximum circular velocities, they nevertheless exhibit a significant dispersion in the final stellar masses and metallicities. Our analysis suggests that this dispersion results from the different accretion histories of the parent dark matter haloes. Statically, we also find evidences to support the Milky Way as a typical Sb/Sc galaxy in the same mass range, providing a suitable benchmark to constrain numerical models of galaxy formation.

Key words: cosmology: theory - galaxies: formation - galaxies: evolution - galaxies: abundances.

1 INTRODUCTION

Our own Galaxy (the Milky Way) has always represented a challenge for galaxy formation theories. Being the only system for which we can access full phase-space information for a significant number of individual stars, the Milky Way represents an important benchmark for theoretical models (Perryman et al. 2001; Beers et al. 2004; Everdasson et al. 1993; Steinmetz et al. 2006; Ivezić et al. 2008). However, it is only one galaxy among many, and may not be representative of ‘typical’ spiral galaxies in the same mass range (Hammer et al. 2007). Hence, a statistical analysis of MW type galaxies could help us to understand to which extent we can rely on the Milky Way to set constraints for galaxy formation models.

The first model for the formation of our Galaxy was proposed by Eggen, Lynden-Bell & Sandage (1962), who argued that the observed relation between the metallicity and the orbital eccentricity of a sample of about 200 stars could be interpreted as a signature of a rapid radial collapse which led to the formation of the stellar halo. Searle & Zinn (1978) later proved this scenario to be inconsistent with the observation of a negligible metallicity gradient for the globular cluster population at large galactocentric distances. These authors proposed an alternative scenario in which the stellar halo of the Galaxy formed through accretion of smaller galactic systems. This picture is in qualitative agreement with expectations from the Cold Dark Matter (CDM) model and with the observed signatures of substructure in the stellar halo of the Milky Way, which appears to be a complex dynamical system still being shaped by merging of smaller neighbouring galaxies (e.g. Vivas & Zinn 2006).

* E-mail: derossi@iafe.uba.ar

Numerical simulations of structure formation in a CDM Universe indicate the important role of the merging histories of dark matter haloes in determining the structure and motions of stars within galaxies. These simulations imply that the last major merger event in our Galaxy should have occurred at $z > 1$, otherwise the very thin cold disc observed in the Galaxy would have been destroyed (Navarro et al. 2004; Kazantzidis et al. 2008). Bekki & Chiba (2001) have also shown that dissipative mergers with gas rich systems could have generated halo stars before the formation of the Galactic disk. More recent studies using an hybrid approach that combines N -body simulations and semi-analytic techniques (Font et al. 2006; De Lucia & Helmi 2008) have suggested that the stellar halo of the Galaxy formed from the accretion of a few relatively massive satellites ($10^8 - 10^9 M_\odot$) at early times (> 9 Gyr).

Although the basic cosmological paradigm appears to be well established, and supported by a large number of observational results, our understanding of the physics of galaxy formation is still far from complete. Within the currently accepted paradigm, galaxies form when gas condenses at the centre of dark matter haloes, which assemble in a ‘bottom-up’ fashion with smaller systems forming first and merging later into larger structures. The evolution of the baryonic components is dominated by complex physical processes (e.g. star formation, supernovae and AGN feedback, chemical enrichment, etc.) which are poorly understood from both the observational and the theoretical viewpoint. The morphology, dynamics and chemistry of a galaxy is the result of many intertwined processes. In this complex framework, a number of questions still remain to be answered: how did the Galaxy assemble? How ‘typical’ is the Galaxy in the Local Universe? Which physical processes play a role in determining its physical and chemical properties? Which kind of merging histories lead to the formation of galactic systems similar to our Galaxy?

In this work we will address some of these questions by taking advantage of one of the largest cosmological simulations of structure formation carried out so far, the Millennium Simulation, which is combined with a semi-analytic model of galaxy formation (for a recent review on these techniques, see Baugh 2006). The aim of this paper is to explore the formation histories of Milky Way-type galaxies and to analyse the origin of the dispersion in their physical properties. In order to achieve this goal we study simultaneously the assembly and chemical evolution of model galaxies, and their location on the well-known correlation between stellar mass and metallicity (e.g. Lequeux et al. 1979; Tremonti et al. 2004; Lee et al. 2006). This strong correlation has been proved to evolve with redshift in such a way that, at a given stellar mass, the gas-phase metallicities of galaxies were lower in the past (e.g. Savaglio et al. 2005; Erb et al. 2006). Studying the evolution of the mass-metallicity relation as a function of cosmic time can provide important information on the physical processes responsible for the joint evolution of the chemical and dynamical properties of galaxies, e.g. supernovae and AGN feedback, star formation and mergers (e.g. Tissera et al. 2005; Brooks et al. 2007; De Rossi et al. 2007; Finlator et al. 2008).

This paper is organised as follows. In Section 2 we give a brief description of the simulation and of the semi-analytic model used in our study. In Section 3 we study the main

physical properties of model Milky-Way type galaxies at $z = 0$, while in Section 4 we study their assembly and formation histories. In Section 5 we analyse the influence of different assembly histories on the chemical properties of model galaxies, as a function of redshift. Finally, we summarise our findings in Section 6.

2 THE NUMERICAL SIMULATION AND THE GALAXY CATALOGUE

This work takes advantage of the Millennium Simulation database¹. The Millennium Simulation (Springel et al. 2005) follows $N = 2160^3$ particles of mass $8.6 \times 10^8 M_\odot h^{-1}$ in a comoving periodic box of 500 Mpc h^{-1} on a side, and with a spatial resolution of 5 kpc h^{-1} in the whole box. The cosmological model is consistent with the first-year data from the Wilkinson Microwave Anisotropy Probe (Spergel et al. 2003): $\Omega_m = 0.25$, $\Omega_b = 0.045$, $h = 0.73$, $\Omega_\Lambda = 0.75$, $n = 1$, and $\sigma_8 = 0.9$. Here, Ω_m , Ω_b and Ω_Λ denote the total matter density, the density of baryons, and dark energy density at $z = 0$, in units of the critical density for closure ($\rho_{\text{crit}} = 3H_0^2/8\pi G$). σ_8 is the rms linear mass fluctuation within a sphere of radius 8 Mpc h^{-1} extrapolated to the present epoch.

The simulation data were stored in 64 snapshots from $z = 127$ to the present day. For each snapshot, dark matter haloes were identified using a standard friends-of-friends (FOF) algorithm with a linking length of 0.2 in units of the mean inter-particle separation. The algorithm SUBFIND (Springel et al. 2001) was used to decompose each FOF group into a set of disjoint substructures. Only substructures retaining at least 20 bound particles (i.e. corresponding to a mass larger than $1.72 \times 10^{10} M_\odot h^{-1}$) were considered genuine and used to construct merger history trees as described in Springel et al. (2005) and De Lucia & Blaizot (2007 - hereafter DLB07). These merger trees represent the basic input to the semi-analytic model that is used to generate the publicly available galaxy catalogues. This methodology was originally introduced by Springel et al. (2001) and De Lucia, Kauffmann & White (2004), and it has been recently updated to include a model for the suppression of cooling flows by ‘radio-mode’ AGN feedback (Croton et al. 2006). A more detailed description of the physical modelling can be found in Croton et al. (2006) and in DLB07.

As illustrated in Fig. 1 in De Lucia et al. (2004), each model galaxy is assumed to be made up of four different baryonic components: (i) *stars*; (ii) *cold gas*, which is available for star formation; (iii) *hot gas*, which is available for cooling and only associated to galaxies sitting at the centre of FOF haloes; and (iv) *ejected gas*, which is made up of material that is temporarily ejected outside the galaxy’s halo by supernovae winds. For the interpretation of the results presented below, it is worth noting that the model adopts an instantaneous recycling approximation (i.e. it neglects the delay between star formation and the recycling of gas and metals from stellar winds and supernovae), and that metals are exchanged between the different components in

¹ A description of the publicly available catalogues, and a link to the database can be found at the following webpage: <http://www.mpa-garching.mpg.de/millennium/>

proportion to the exchanged mass (for details, see De Lucia et al. 2004). In addition, the model assumes that all metals produced by new stars are instantaneously mixed with the available cold gas (i.e. the model assumes a 100 per cent mixing efficiency).

Finally, we remind the reader that the model used in this study follows dark matter substructures explicitly, i.e. the haloes within which galaxies form are still followed after they are accreted onto larger systems. This scheme leads to three different types of galaxies: Central galaxies of FOF groups are referred to as ‘type 0’, and are the only galaxies fed by gas that is cooling radiatively from the surrounding halo. Galaxies attached to distinct dark matter substructures are called ‘type 1’, and their orbits are followed by tracking the parent dark matter substructure until tidal stripping reduces its mass below the resolution of the simulation (De Lucia et al. 2004; Gao et al. 2004). The galaxy at the centre of the dissolving substructure is not affected by tidal stripping, and is assigned a merging time using the classical dynamical friction formula. These galaxies are referred to as ‘type 2’.

3 THE SAMPLE OF GALAXIES

In this work, we defined as Milky Way (MW) type galaxies those type 0 systems which inhabit haloes with $200 < V_{\max} < 250 \text{ km s}^{-1}$ (Li & White 2008), where V_{\max} is the maximum circular velocity, which is estimated directly from the simulation. This selection provides a total of 130311 systems, which is consistent with the number of L^* galaxies estimated from the observed local luminosity function. We also restricted the sample to galaxies with $1.5 < \Delta M < 2.6$ with $\Delta M = M_{\text{bulge}} - M_{\text{total}}$ (M_{bulge} and M_{total} are the bulge and total magnitude in the B-band), so as to select galaxies with an Sb/Sc morphology (Simien & de Vaucouleurs 1986). The final sample used in this study is made up of 52149 systems that we called MW type galaxies. We choose the maximum circular velocity and the morphological type to select MW haloes because these two physical properties are observationally better determined than the total stellar mass and cold gas fraction, for example. We also extend the analysis including observational estimates on these two parameters and refer to this sample as a restricted MW sample (RMWS). Adopting $f_g = 0.088 \pm 0.019$ and $M_* = (4.75 \pm 1.1)10^{10} M_{\odot} h^{-1}$ (Guesten & Mezger 1982; Kulkarni & Heiles 1987; Boissier & Prantzos 1999; Lineweaver 1999; De Lucia & Helmi 2008), we find that 10.7% of the total model MW type galaxies would constitute a closer representation of our own Galaxy.

In Fig. 1, we show the distributions of total stellar masses (M^*), cold gas fractions (f_{cold}), and stellar mass-weighted ages for our model MW type galaxies. The cold gas fraction is defined here as $\frac{M_{\text{gas}}^{\text{cold}}}{M_{\text{gas}}^{\text{cold}} + M^*}$, where $M_{\text{gas}}^{\text{cold}}$ is the cold gas mass of the system. The shaded regions in each panel show the available observational estimates for our Galaxy (i.e. Guesten & Mezger 1982; Kulkarni & Heiles 1987; Boissier & Prantzos 1999; Lineweaver 1999; De Lucia & Helmi 2008)². The distributions shown in Fig. 1 peak

close to these observational estimates, but also exhibit a large dispersion. This shows that, although galaxies have been selected to have a narrow range of circular velocities (i.e. total mass), they had significantly different evolutionary histories, which produced the relatively large scatter in stellar mass and gas content visible in Fig. 1.

In Fig. 2, we show the cold gas-phase metallicity as a function of the stellar mass for the model MW type galaxies used in this study (contours). Symbols with error bars indicate the mean and standard deviation of the distribution. For comparison, we have also plotted the mass-metallicity relation (MZR) for the full galaxy catalogue (the solid line indicate the mean, and the dashed lines the scatter of the distribution). Fig. 2 shows that there is a well defined correlation between the gas-phase metallicity and the stellar mass. The gas-phase metallicity increases approximately linearly for stellar masses below $\sim 10^{11} M_{\odot} h^{-1}$, and flattens for more massive galaxies, remaining constant about the solar value. Model MW type galaxies are located around the turnover of the Millennium MZR. Their mean metallicity grows with stellar mass with a slightly steeper slope compared to the general trend of the Millennium MZR, but with similar slope to that reported by Tremonti et al. (2004) for the observed MZR of star forming galaxies in the SDSS. Model MW type galaxies show a standard deviation of ~ 0.10 dex, which is comparable to that estimated by Tremonti et al. We note that the relatively large dispersion of the observed relation cannot be entirely explained by observational uncertainties. In a recent work, Cooper et al. (2008) suggested that part (about 15 per cent) of the scatter in the MZR could be explained by environmental differences. The model relation shown in Fig. 2 includes galaxies in all environments (from field to clusters), and the metallicities have not been convolved with typical observational uncertainties.

The MZR reflects the balance between star formation activity and other physical processes such as Supernovae and AGN feedbacks, environmental effects, etc. Studying the origin of this relation and of its dispersion can therefore provide important information of the sequence of events which led to the formation of galaxies similar to our own Milky Way. In the following, we will analyse the origin of the MZR of model MW type galaxies by studying their assembly and chemical enrichment histories simultaneously.

4 THE ASSEMBLY OF MODEL GALAXIES

We constructed the full galaxy merger trees for all our model MW type galaxies and analysed them as in DLB07. We remind the reader that, among the different ‘branches’ of a galaxy merger tree, the ‘main branch’ is special, because it connects a galaxy to its most massive progenitor (the ‘main progenitor’) at each node of the tree. In the following, we will refer to all mergers onto the main branch as ‘accretion events’. Major mergers correspond to accretion events in which the stellar mass of the accreted galaxy is at least one third of the stellar mass in the main progenitor at the time of accretion.

² Note that while the mean ages of model MW galaxies were calculated considering the whole stellar component, the observed values correspond only to the old thin disk of the Galaxy.

² Note that while the mean ages of model MW galaxies were

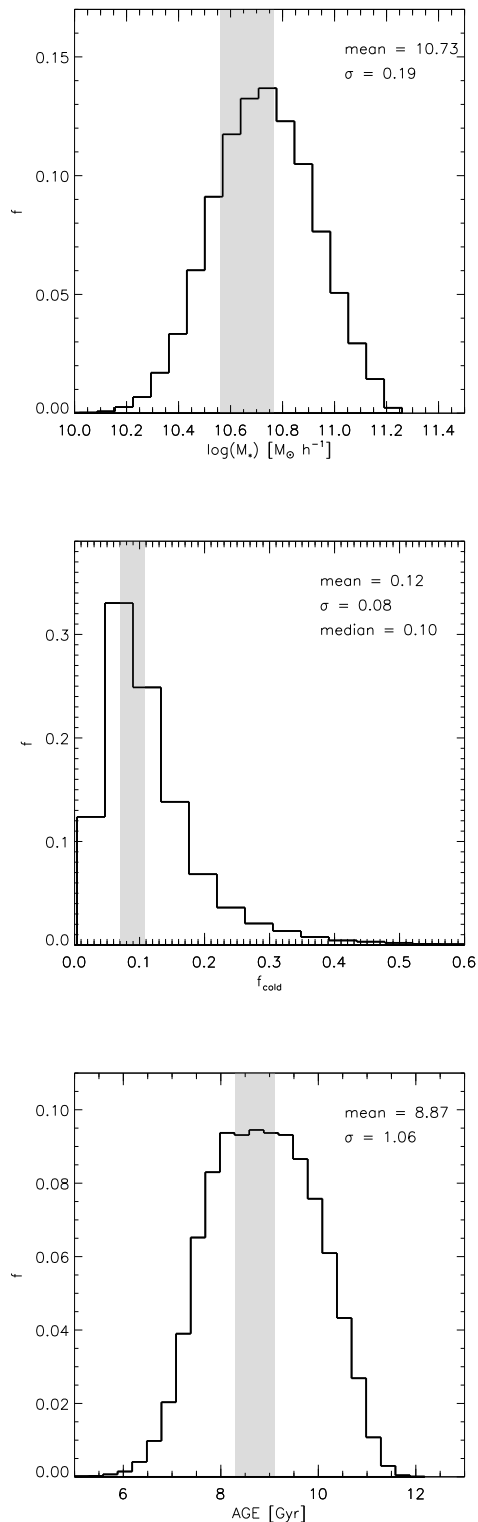


Figure 1. Distributions of stellar masses, cold gas fractions and stellar mass-weighted ages for the model MW type galaxies used in this study. The shaded regions correspond to the observational values for our Galaxy. See De Lucia & Helmi 2008, and references therein. For the stellar age, an accurate total observational estimate is not available. For this quantity (bottom panel) we have plotted the range corresponding to the old thin disk by Lineweaver (1999).

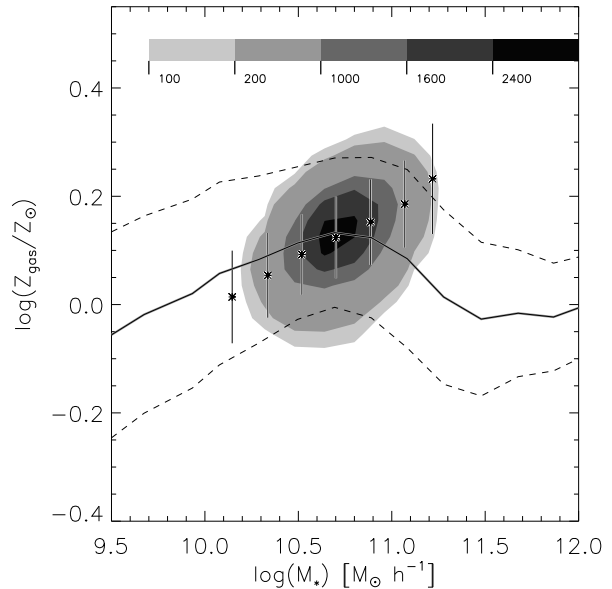


Figure 2. Cold gas-phase metallicity as a function of the stellar mass for the model MW type galaxies used in this study (contours), and for the full Millennium galaxy catalogue by DLB07 (solid line). The colour-coding of the contours indicate the mean number of galaxies in a bin of 0.15 dex in stellar mass and 0.03 dex in metallicity. Mean values and their standard deviations for the MW type galaxies are shown as symbols with error bars. Dashed lines indicate the dispersion in the Millennium MZR.

For the Millennium simulation, Springel et al. (2005) found that the halo mass function can be reliably estimated down to 20 particles. Moreover, De Lucia & Helmi (2008) presented a complete study of numerical convergence for the semi-analytic model adopted in this work. These authors built up galaxy merger trees and studied the physical properties of the structure along them, in four realization of the same initial condition but with increasing numerical resolution. Their results indicate a very good level of convergence for the range of particle mass of few 10^8 to $10^5 M_\odot h^{-1}$. These previous studies provide evidences that for the mass range studied in this work, merger trees and the properties of galaxies along them are reliably estimated.

For our MW type sample, only a small fraction of the final stellar mass is formed in the accreted systems. This can be seen in the top left panel of Fig. 3 which shows the total stellar mass acquired through mergers, normalised to the final stellar mass of the galaxy. At $z = 0$, the total accreted stellar mass varies between ~ 7 and ~ 23 per cent of the final stellar mass, with a mean value of ~ 15 per cent. Most of the accretion occurs relatively late, with only ~ 5 per cent of stellar mass accreted before $z \sim 1$. The dashed region in the top left panel of Fig. 3 shows the fraction of cold gas accreted through mergers as a function of lookback time, again normalised to the final stellar mass. This represents only ~ 6 per cent of the final stellar mass. The figure shows then that about 80 per cent of the stars in our MW type sample formed *in situ* in the main progenitors. Galaxies in

the RWMS tend to have more important accretion events, particularly at $z \lesssim 0.5$, but differences with respect to the main sample are very small (less than 10%).

The top right panel of Fig. 3 shows the mean evolution of the stellar mass in the main progenitor, as a function of lookback time (solid line), and the mean evolution of the total stellar mass already formed (i.e. the sum of the stellar mass in all progenitors at a given time, dashed line). The dashed and shaded regions show the scatter of the distributions. At $z \sim 1$, about 60 per cent of the total stellar mass is already in place in a single object, both for the main and the restricted sample. Accounting for the stellar mass in all other progenitors does not change these numbers significantly.

The results shown in the top panels of Fig. 3 therefore demonstrate that the evolution traced by following the main branch provides a good representation of the evolution of our MW type galaxies. As discussed above, most of the stars in the final systems are formed *in situ* through the transformation of gas that comes primarily from infall. The mean evolution of the cold gas component is shown in the bottom left panel of Fig. 3. The shaded region shows the scatter of the distribution. The figure shows that mean gas fraction in the main branch declines from ~ 0.8 at $z \sim 5$ to ~ 0.10 at present. At $z = 2$, the gas fraction is ~ 0.5 , in qualitative agreement with gas fractions measured by Erb et al. (2006) for a sample of UV selected galaxies. At $z=0$, our typical MW type galaxy has a gas fraction varying between ~ 0.05 and 0.20 , with a mean value of 0.12 (Fig. 1). The trend is similar for galaxies in the RMWS, but they exhibit a more rapid gas consumption between $z \sim 1.5$ and $z \sim 0.5$.

The decrease of the available gas results in a decrease of the mean star formation rate by about a factor of 10 between $z \sim 2$ and $z \sim 0.45$. The mean value of the star formation rate at present is about $1.89 M_{\odot} \text{yr}^{-1}$, which is slightly higher than the $\lesssim 1 M_{\odot} \text{yr}^{-1}$ observational estimates for our Galaxy (e.g. Guesten & Mezger 1982; Kulkarni & Heiles 1987; Boissier & Prantzos 1999; Just & Jahreiss 2007). The bottom right panel of Fig. 3 shows the mean evolution of the specific star formation rate. This exhibits a large spread, particularly at low redshifts, indicating that a significant fraction of our MW galaxies have decreased their star formation activity during the last ~ 6 Gyrs. These effects are slightly stronger for galaxies in the RMWS (inset plot), which end having star formation rates around $\sim 0.26 M_{\odot} \text{yr}^{-1}$, which are now a bit lower than the observational estimations for our Galaxy.

This is (at least in part) due to the strong AGN feedback adopted in the model in order to suppress cooling flows in relatively massive haloes. This strong AGN feedback, combined with a relatively strong supernovae feedback in this particular mass range, seems to exhaust the gas available for star formation on relatively short time scales (see also discussion in Sec. 6.1 of DLB07 for the brightest cluster galaxies). A possible solution to this issue might be the implementation in the model of a new mechanism capable of re-activating cooling flows at later times but this analysis is out of the scope of this work.

Only a small fraction (about 12 per cent) of galaxies in our MW type sample suffered at least one major merger event during its life, i.e. all objects accreted onto the main branch have mass smaller than a third the mass of the main progenitor at the time of the merger event. A more de-

tailed investigation showed that most of the major mergers occurred at $z > 1$, and that only 3.23 per cent of MW type galaxies had a major merger as their last accretion event. These results do not change significantly for galaxies in RMWS. Therefore, our MW galaxies have a relatively quiet life with no important mergers and a number of minor accretion events that only add a relatively small fraction of the total final mass.

In Fig. 4 we show the evolution of each of the baryonic phases (see Sec. 2) associated to our MW galaxies as a function of lookback time. Note that the vertical axis has been plotted using logarithmic scale. It is clear that at lower redshifts most of the baryons are in the hot and stellar phases, while the cold and ejected gas components dominate at very high redshifts. In particular, the ejected mass reaches a maximum at $z \approx 2.6$. In the case of cold gas mass, it has a maximum at $z \sim 1.5$, when f_{cold} is around 0.4. Similar results are obtained for galaxies in the RMWS. In particular, the median cold gas mass at $z = 0$ for the RMWS is approximately $6 \times 10^9 M_{\odot}$, in good agreement with observations (Blitz 1997 and references therein). At $z < 3$ we estimate quite large hot gas masses. This in part due to the cooling flow suppression by AGN feedback used to build up the galaxy catalogue. Croton et al. (2006) tuned the model to reproduce the local relation between the mass of the bulge and the mass of the black hole and it is known that the MW black hole is offset from this relation. Then, as expected, for our MW type galaxies we obtained a mean central black hole mass of $\sim 4.8 \times 10^7 M_{\odot} h^{-1}$, which is one order of magnitude above the observational estimations for the Milky Way galaxy (Schödel et al. 2002). Also Supernova feedback contributes to build up the hot phase. Although at lower redshifts supernovae are not the main source of heating, the excess of hot gas might suggest that the combination of both type of feedbacks and their relative importance need to be revised. Finally, we note that recent observational studies have shown evidence for the existence of hot halo gas surrounding spiral galaxies (Pedersen et al. 2006).

5 CHEMICAL EVOLUTION OF MODEL GALAXIES

In the previous sections, we have studied the global properties of model MW galaxies, focusing on their assembly and merger histories. In this section, we will see how these histories influence the chemical evolution of MW galaxies and their location on the mass-metallicity relation.

In Fig. 5 we show the MZR for the main progenitors of model MW galaxies at different redshifts. The distribution of galaxies in this diagram is shown using contours, which have been coded as a function of the cold gas fraction, f_{cold} . Symbols with error bars show the mean and dispersion of the distributions. As a reference, we also plot the mean Millennium MZR (solid line) at $z = 0$.

At high redshift, the MW progenitors cover a wider range of stellar masses (~ 3 dex) and metallicities (~ 1.5 dex) than the model MW galaxies at $z = 0$. Some progenitors reach gas-phase metallicities of around solar or even super-solar values at $z \sim 3$, while others have significantly sub-solar values. Fig. 5 also shows that most of the evolution in the metallicities of the progenitors occurs at $z > 1$. Be-

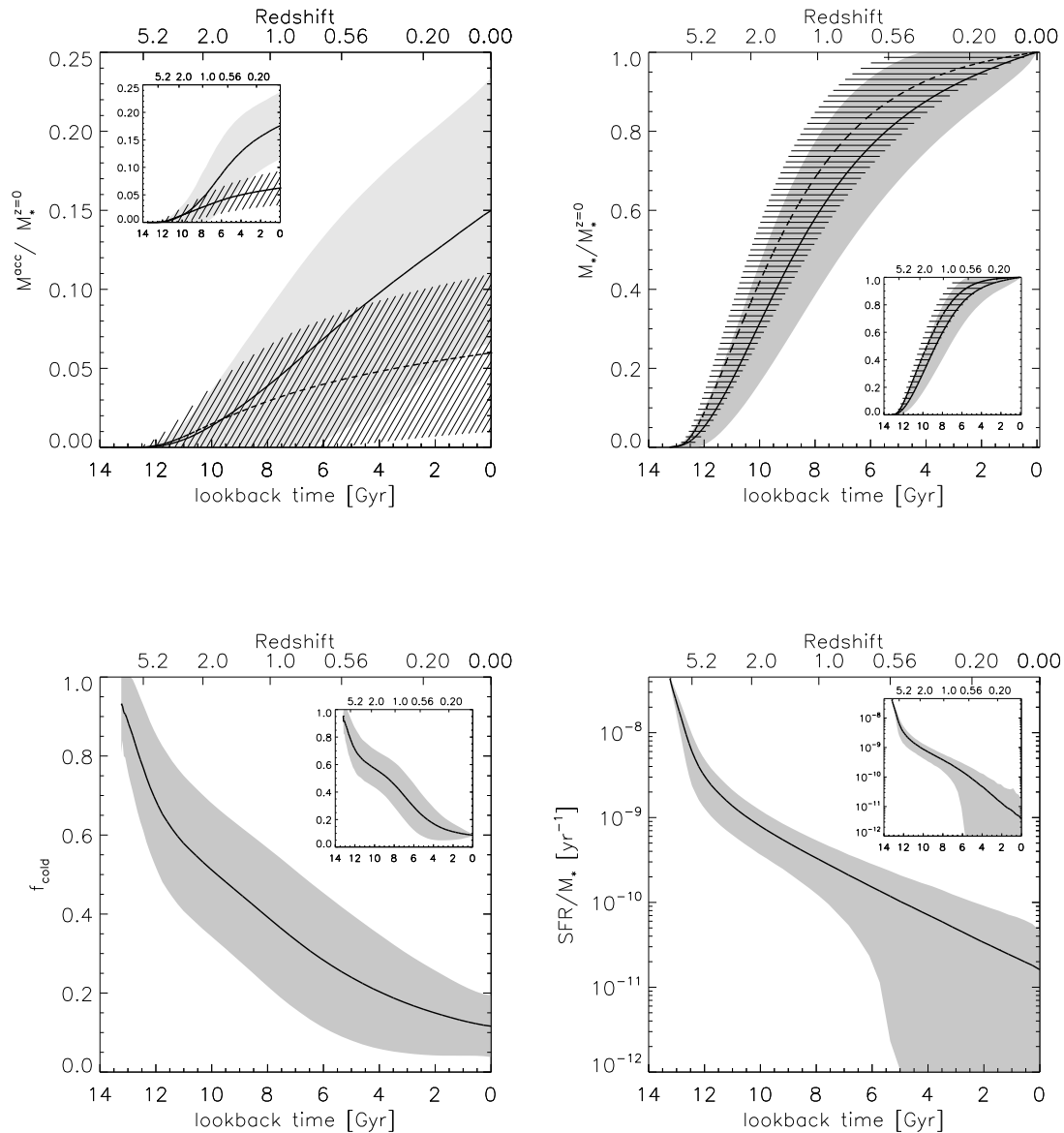


Figure 3. Top left panel: stellar mass (solid line) and cold gas mass (dashed line) accreted through mergers onto the main branch as a function of lookback time, normalised to the final stellar mass at $z=0$. Top right panel: mean evolution of the stellar mass in the main branch (solid line) and of the total stellar mass in all progenitors at any given time (dashed line). Lower left panel: mean evolution of the cold gas fraction in the main branch. Lower right panel: mean evolution of the specific star formation rate in the main branch. In all panels, shaded (and dashed regions when present) indicates the $1\text{-}\sigma$ dispersion of the distributions. The inset plots correspond to the results for the RMWS defined by imposing systems to fulfill constraints on stellar masses and cold gas fractions similar to our Galaxy.

low this redshift, the distribution shrinks significantly and the mean stellar mass of MW progenitors is typically larger than 60 per cent of the final stellar mass of the systems (see also Fig. 3 and relative discussion).

As discussed in the previous section, the star formation rate in the main progenitors of the model MW galaxies is tightly related to the availability of cold gas as expected. Both of them regulates the chemical enrichment of the systems. At $z \approx 3$ our results show that less massive (which are

also less enriched) systems have, on average, larger cold gas fractions and higher star formation rates. More massive systems have lower gas fractions and star formation rates, which prevents further enrichment (Fig. 5). The largest changes in metallicity occur for those systems which have the lowest stellar masses (and consequently, the highest gas fractions) at high redshift. These galaxies exhibit an increase in metallicity of ~ 0.2 dex since $z = 1$. Galaxies in the RMWS

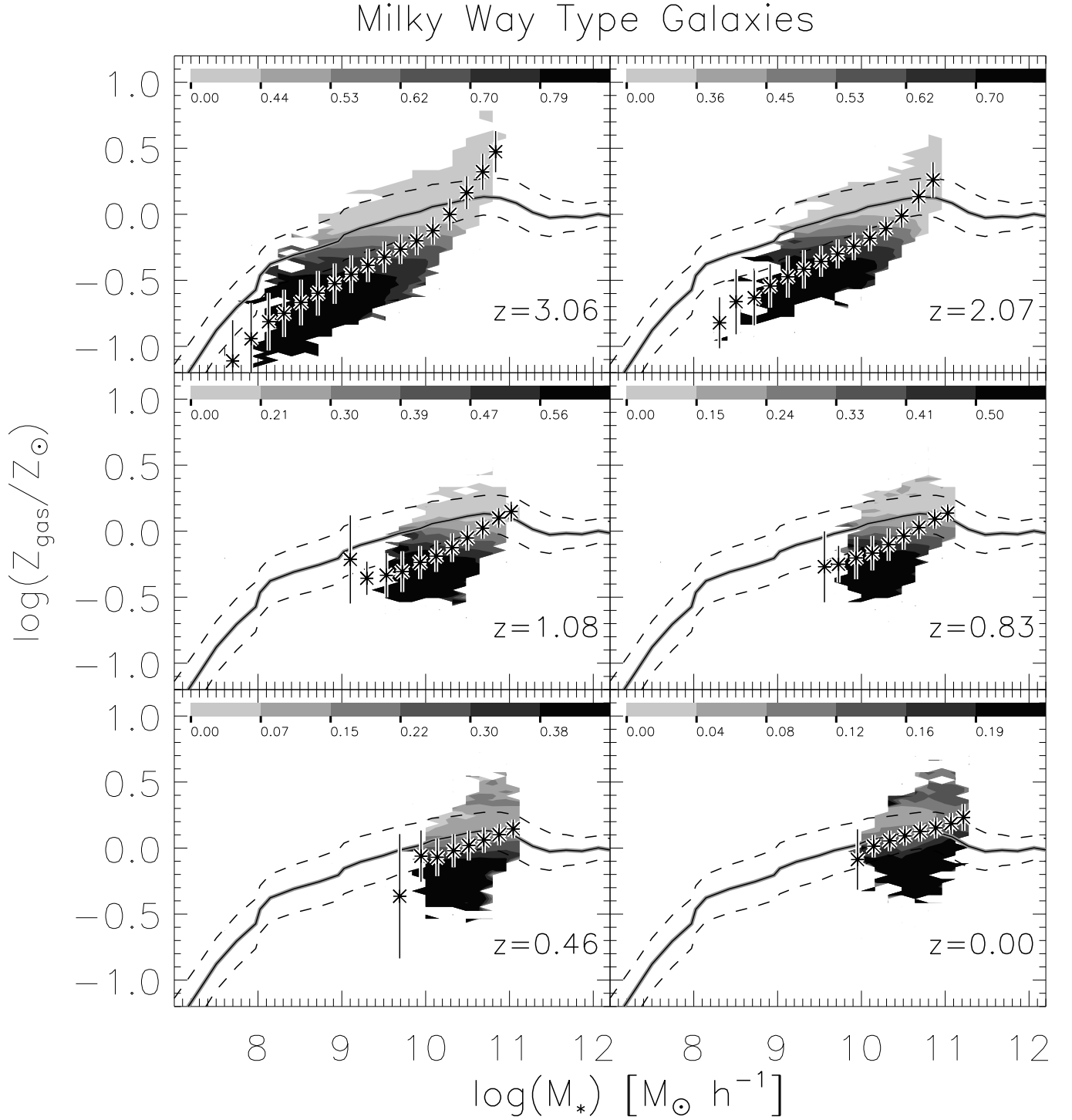


Figure 5. Evolution of the MZR for galaxies in our MW sample. At $z > 0$, we plot the gas-phase metallicity and stellar mass of the main progenitor of each galaxy in the local sample. Contour levels are colour-coded according to the cold gas fraction. In each panel, we also show the mean (solid line) relation for all galaxies in the catalogue at $z = 0$, and its dispersion (dashed lines).

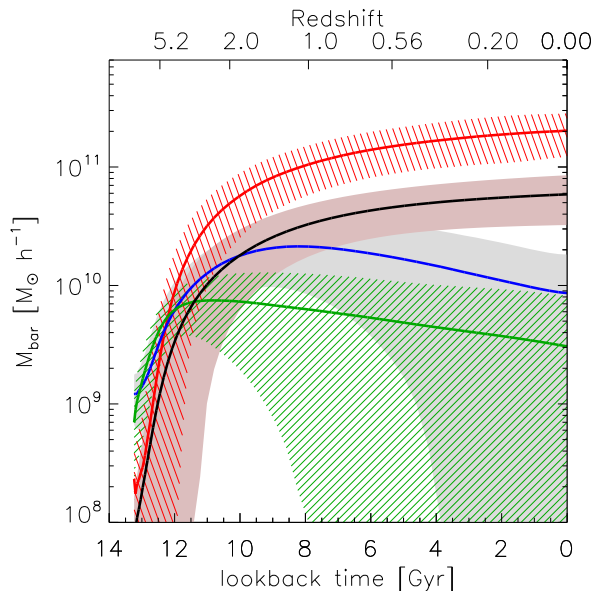


Figure 4. Evolution of baryonic mass for MW main progenitors. Note that the vertical axis has been plotted using logarithmic scale. The solid lines depict the mean relations for the different baryonic phases: cold gas (blue), ejected mass (green), hot gas (red) and stars (black). The shaded and dashed areas represent the standard deviations.

exhibit the same general behavior, but covering a smaller parameter range in the MZ-plane as expected.

In Fig. 6 we show the mean fraction of mass accreted as a function of lookback time for objects with large (left panel) and small (right panel) gas fractions at $z \sim 3$. Gas-rich progenitors ($f_{\text{cold}} > 0.8$) not only have larger than average star formation rates, but also have accreted a factor of two more stellar mass than gas-poor progenitors ($f_{\text{cold}} < 0.4$), leading to more rapid chemical enrichment. Conversely, progenitors that are gas-poor at $z \sim 3$ do not evolve significantly in metallicity; they have completed most of their accretion already at high redshifts (right panel of Fig. 6).

The results discussed above indicate that the large dispersion in metallicity and stellar mass of our MW galaxies is related to the intrinsic dispersion in the mass accretion histories of the haloes hosting MW type galaxies at $z = 0$. Our MW type galaxies were selected to lie in a narrow range of circular velocities (i.e. total masses) and morphologies. Our results show that this selection gives rise to a sample of galaxies with a relatively wide range of stellar masses and metallicities, and that the scatter can be related to the assembly and gas accretion histories of the parent haloes. The halo mass thus does not uniquely determine the properties of the galaxies they host. This is confirmed in Fig. 7 which shows the distribution of virial masses of haloes hosting the gas-rich and gas poor MW progenitors at $z \sim 3$. As we can see, the two types of progenitors inhabit different mass haloes at high redshift, although they end up in haloes of similar mass at the present day.

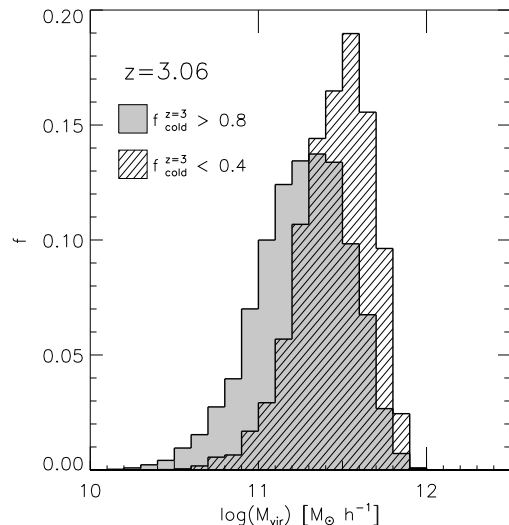


Figure 7. Distribution of virial masses of the main progenitors of MW type galaxies, at $z \sim 3$. Shaded histograms are for systems with cold gas fraction > 0.8 , while the dashed histograms are for systems with cold gas fraction < 0.4 at the same redshift.

6 CONCLUSIONS

In this paper we have studied the assembly and chemical evolution of MW type galaxies. We used the galaxy catalogue built by DLB07 for the Millennium Simulation, and selected MW type galaxies by imposing circular velocity and bulge-to-disk ratio constraints. Our model MW type galaxies have mean properties such stellar mass, gas fraction, age and star formation rate, in good agreement with the estimations obtained for our own Galaxy. Interestingly, there is also substantial dispersion in these quantities which, according to our work, can be related to their history of assembly.

Taking advantage of the publicly available database of merger trees, we studied the assembly and chemical enrichment histories of our model MW type galaxies. Our main results can be summarised as follows:

1. Most of the final stellar mass of model MW type galaxies is formed *in situ* from gas infalling from the surrounding halo. A small fraction of the final stellar mass (about 15 per cent) is formed in smaller galaxies that are accreted over the lifetime of the Milky Way. Only 12 per cent of our model MW type galaxies experienced a major merger during their lifetime, and for only 3.23 per cent of our sample was this major merger the last accretion event.

2. The distribution of baryons in different components is regulated by feedback processes. At $z > 4$, supernovae feedback is effective in ejecting large fractions of the gas outside the haloes (due to the shallower potential wells). By $z \sim 1$, a large part of this gas has been re-incorporated and the suppression of cooling flows by AGN feedback starts playing a more important role, keeping an important fraction of the baryons in the hot phase.

3. The MZR of model MW type galaxies has a dispersion of ~ 0.10 dex, in agreement with the observed results by Tremonti et al. (2004). We found that, at a given stel-

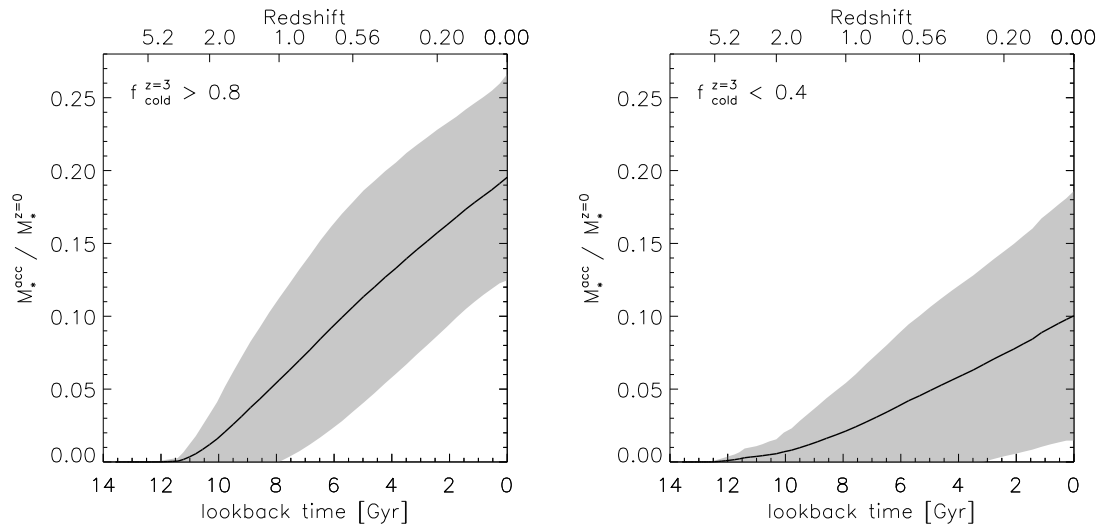


Figure 6. Evolution of the total accreted stellar mass for the main progenitors of MW type galaxies, normalised to final stellar mass at $z = 0$. The left panel is for progenitors with cold gas fraction > 0.8 at $z \sim 3$, while the right panel is for progenitors with cold gas fraction < 0.4 at the same redshift.

lar mass, the main parameter determining this dispersion is the gas richness of the systems. Gas-rich systems tend to be more metal-poor, while gas-poor galaxies have converted most of their cold gas component into stars in the past and, therefore have reached a higher level of chemical enrichment.

4. The accretion histories of the haloes hosting our MW type galaxies exhibit a large dispersion. Haloes hosting gas-rich MW progenitors at high redshifts tend to experience a higher accretion rate at later times. These differences in the accretion histories of the parent haloes introduce differences in the star formation rates of the progenitors which, on their turn, modulate the impact of supernovae and AGN feedbacks. This leads to an important dispersion in the stellar masses and metallicities of the $z=0$ Milky Way systems.

5. If we restrict the model MW galaxies to satisfy also observational constraints on stellar mass and gas fractions, we get a smaller sample with similar trends to those of the complete MW type sample reflecting the fact that the dark matter halo is the dominant factor determining the history of assembly of galaxies. However, the dispersion in the metallicity and gas fraction at a given mass is produced by slightly differences in the accretion rates of substructures which regulate the star formation activity.

Our findings suggest that part of the dispersion observed in the MZR could be revealing differences in the histories of formation. Also, our results suggest that the Galaxy may be consider a typical Sb/Sc galaxy in the same mass range, providing a suitable benchmark for numerical models of galaxy formation.

ACKNOWLEDGEMENTS

We thank the anonymous referee for her/his useful comments that largely helped to improve this paper. This work was partially supported by the European Union’s ALFA-II programme, through LENAC, the Latin American European Network for Astrophysics and Cosmology. We acknowledge support from Consejo Nacional de Investigaciones Científicas y Técnicas and Agencia de Promoción de Ciencia y Tecnología. The Millennium Simulation databases used in this paper and the web application providing online access to them were constructed as part of the activities of the German Astrophysical Virtual Observatory.

REFERENCES

- Baugh C. M., 2006, RPPh, 69, 3101
 Beers T. C., et al., 2004, IAUS, 220, 195
 Bekki K., Chiba M., 2001, ApJ, 558, 666
 Benson A. J., Bower R. G., Frenk C. S., White S. D. M., 2000, MNRAS, 314, 557
 Blitz L., 1997, IAUS, 170, 11
 Boissier S., Prantzos N., 1999, MNRAS, 307, 857
 Brooks A. M., Governato F., Booth C. M., Willman B., Gardner J. P., Wadsley J., Stinson G., Quinn T., 2007, ApJ, 655, L17
 Cooper M. C., Tremonti C. A., Newman J. A., Zabludoff A. I., 2008, MNRAS, 390, 245
 Croton D. J., et al., 2006, MNRAS, 365, 11
 De Lucia G., Kauffmann G., White S. D. M., 2004, MNRAS, 349, 1101
 De Lucia G., Springel V., White S. D. M., Croton D. J., 2006, MNRAS, 366, 499
 De Lucia G., Blaizot J., 2007, MNRAS, 375, 2
 De Lucia G., Helmi A., 2008, MNRAS, 391, 14
 de Rossi M. E., Tissera P. B., Scannapieco C., 2007, MNRAS, 374, 323

- Edvardsson B., Andersen J., Gustafsson B., Lambert D. L., Nissen P. E., Tomkin J., 1993, *A&AS*, 102, 603
- Eggen O. J., Lynden-Bell D., Sandage A. R., 1962, *ApJ*, 136, 748
- Erb D. K., Shapley A. E., Pettini M., Steidel C. C., Reddy N. A., Adelberger K. L., 2006, *ApJ*, 644, 813
- Erb D. K., Steidel C. C., Shapley A. E., Pettini M., Reddy N. A., Adelberger K. L., 2006, *ApJ*, 646, 107
- Finlator K., Davé R., 2008, *MNRAS*, 385, 2181
- Font A. S., Johnston K. V., Bullock J. S., Robertson B. E., 2006, *ApJ*, 638, 585
- Gao L., White S. D. M., Jenkins A., Stoehr F., Springel V., 2004, *MNRAS*, 355, 819
- Guesten R., Mezger P. G., 1982, *VA*, 26, 159
- Hammer F., Puech M., Chemin L., Flores H., Lehnert M. D., 2007, *ApJ*, 662, 322
- Ivezic Z., et al., 2008, *ApJ*, 684, 2871
- Just A., Jahreiss H., 2007, arXiv, arXiv:0706.3850
- Kazantzidis S., Bullock J. S., Zentner A. R., Kravtsov A. V., Moustakas L. A., 2008, *ApJ*, 688, 254
- Kulkarni S. R., Heiles C., 1987, *ASSL*, 134, 87
- Lee H., Skillman E. D., Cannon J. M., Jackson D. C., Gehrz R. D., Polonski E. F., Woodward C. E., 2006, *ApJ*, 647, 970
- Lequeux J., Peimbert M., Rayo J. F., Serrano A., Torres-Peimbert S., 1979, *A&A*, 80, 155
- Li Y.-S., White S. D. M., 2008, *MNRAS*, 384, 1459
- Lineweaver C. H., 1999, *Sci*, 284, 1503
- Maller A. H., 2005, *pgqa.conf*, 237
- Moore B., Davis M., 1994, *MNRAS*, 270, 209
- Navarro J. F., 2004, *ASSL*, 319, 655
- Pedersen K., Rasmussen J., Sommer-Larsen J., Toft S., Benson A. J., Bower R. G., 2006, *NewA*, 11, 465
- Perryman M. A. C., et al., 2001, *A&A*, 369, 339
- Savaglio S., et al., 2005, *ApJ*, 635, 260
- Searle L., Zinn R., 1978, *ApJ*, 225, 357
- Schödel R., et al., 2002, *Natur*, 419, 694
- Simien F., de Vaucouleurs G., 1986, *ApJ*, 302, 564
- Spergel D. N., et al., 2003, *ApJS*, 148, 175
- Springel V., et al., 2005, *Natur*, 435, 629
- Steinmetz M., et al., 2006, *AJ*, 132, 1645
- Tissera P. B., De Rossi M. E., Scannapieco C., 2005, *MNRAS*, 364, L38
- Tremonti C. A., et al., 2004, *ApJ*, 613, 898
- Vivas A. K., Zinn R., 2006, *AJ*, 132, 714
- Wang Q. D., Immler S., Walterbos R., Lauroesch J. T., Breitschwerdt D., 2001, *ApJ*, 555, L99